*Pure Appl. Chem.*, Vol. 74, No. 10, pp. 1811–1821, 2002.


# Sea-water solubility phase diagram. Application to an extractive process*

R. Cohen-Adad[1,‡], Chr. Balarew[2], S. Tepavitcharova[2], and D. Rabadjieva[2]

*[1]Université Claude Bernard Lyon I, 43 Boulevard du 11 Novembre 1918, 69622 Villeurbanne Cedex, France; [2]Institute of General and Inorganic Chemistry, Bulgarian Academy of Sciences, Acad. G. Bontchev Str., Bl. 11, 1113 Sofia, Bulgaria*

*Abstract*: The main goal of this presentation is to tentatively forecast or improve an extractive process. The sea-water system is described using a graphical representation of the quinary ion-pair system $Na^+$, $K^+$, $Mg^{2+}$/ $Cl^-$, $SO_4^{2-}$// $H_2O$. The operations required by extraction or purification of a sea-water component are simulated by a path through the solubility diagram. The procedure is applied to isothermal evaporation of Black Sea water at 25 °C, and the balance of the crystallization sequence is determined. In the same way, the cooling of residual brine, after precipitation of pure sodium chloride, is studied.

## INTRODUCTION

A path through the solubility diagram allows the simulation of any operation required for the separation of a component from sea water or its purification. It is, therefore, of major interest for the conception or improvement of an extractive process, but in spite of the great number of available data in literature, the sea-water system is still under-exploited, due to the complexity of the system or to the lack of reliable data in some solubility fields. The principles of computer-assisted calculation of brine crystallization, based on solubility data, have been presented in previous publications, and the investigations were developed in several directions:

- Critical evaluation of multicomponent systems [2–8]
- Calculation of crystallization sequence [9,10]
- Recovery of some salts contained in sea water [12,13]
- Preparation of software [14,15]

The main goal of this presentation is to tentatively forecast an extractive process, and the calculations have been performed with Black Sea water.

## SEA-WATER SYSTEM (REVIEW OF MAIN PROPERTIES)

The sea-water solubility phase diagram is very complex since it involves almost all elements of the periodic classification and many compounds are observed during a crystallization sequence. Some components (major elements) precipitate during evaporation or cooling, whereas the solubility product of the others (minor and trace elements) is not reached and they remain almost completely in the liquid phase.

*Lecture presented at the 10th International Symposium on Solubility Phenomena, Varna, Bulgaria, 22–26 July 2002. Other lectures are published in this issue, pp. 1785–1920.

‡Corresponding author

Consequently, the study and the representation of phase equilibria can be simplified and described in the frame of a quinary system [8–10]:

$$Na^+, K^+, Mg^{2+}/ Cl^-, SO_4^{2-}// H_2O$$

## Expression of composition

Cooling, heating, evaporation, or addition of a reactant are the main techniques used for an extractive treatment of sea water, and during treatment, the content of minor and trace elements increases progressively so that they must be taken in account in the expression of composition. An unsymmetrical expression of composition is desirable in order to get a suitable representation of sea water, and the Jänecke expression [1], taking into account the charge of ions, has been found to be the most convenient.

$$X_i = 100z_in_i/D, \quad Y_j = 100z_jn_j/D \quad Z = 100n_{H_2O}/D \quad D = \Sigma\, z_in_i = \Sigma\, z_jn_j \tag{1}$$

In eq. 1, $i$ and $j$ are related to all cations and anions of the brine (including minor and trace elements), $n$ and $z$ are, respectively, the amount and the charge of a component; $D$ is the moles number of the solution extended over all anions or cations, taking into account their charge in order to satisfy the electroneutrality condition of the medium.

## Graphical representation

Under isobaric-isothermal conditions, the sea-water system involves four composition variables ($X_K$, $X_M$, $Y_S$, $Z$), and its graphical representation requires, in a three-dimensional space, two graphs, one for the salt composition and one for the water content. Each graph is a volume [9–11] and has, at 25 °C, 15 faces where a second solid phase precipitates together with NaCl, 32 edges where two solid phases coprecipitate with NaCl, and 26 apices where four solid phases are in equilibrium with saturated solution. The chemical formula, name, symbol, and crystallization field of all solid phases coprecipitating with NaCl at 25 °C are presented in Table 1. The composition of the apices and the name and nature of the observed solid phases are given in Table 2.

**Table 1** Sea-water system: main observed compounds at 25 °C.

| Symbol | Name | Formula | Crystallization field |
|---|---|---|---|
| NC | Halite | $NaCl$ | |
| KC | Sylvinite | $KCl$ | mnpqe |
| MC6 | Bischoffite | $MgCl_2{\cdot}6H_2O$ | aldz |
| NS | Thenardite | $Na_2SO_4$ | shcg |
| MS1 | Sakeite (Kieserite) | $MgSO_4{\cdot}H_2O$ | xykj |
| MS4 | Leonhardite | $MgSO_4{\cdot}4H_2O$ | ykldr |
| MS6 | Hexahydrite | $MgSO_4{\cdot}6H_2O$ | jkyx |
| MS7 | Epsomite | $MgSO_4{\cdot}7H_2O$ | vijxw |
| KMC6 | Carnallite | $KCl{\cdot}MgCl_2{\cdot}6H_2O$ | eqrdz |
| N3KS | Glaserite | $Na_2SO_4{\cdot}3K_2SO_4$ | fgstm |
| NMS4 | Astrakanite | $Na_2SO_4{\cdot}MgSO_4{\cdot}4H_2O$ | ihstuv |
| KMS4 | Leonite | $K_2SO_4{\cdot}MgSO_4{\cdot}4H_2O$ | unpwv |
| KMS6 | Schönite | $K_2SO_4{\cdot}MgSO_4{\cdot}6H_2O$ | tumn |
| KMCS3 | Kaïnite | $KCl{\cdot}MgSO_4{\cdot}3H_2O$ | wpqryx |

**Table 2** Solubility of NaCl at 25 °C: apices of the phase diagram.

| | XK | XM | YS | Z | Solid phases |
|---|---|---|---|---|---|
| c | 0 | 0 | 20.21 | 802 | NS |
| h | 0 | 25.29 | 28.9 | 762 | NS + NMS4 |
| s | 14.25 | 22.15 | 30.72 | 694 | NS + NMS4 + N3KS |
| t | 14.38 | 47.94 | 25.34 | 685 | NMS4 + N3KS + KMS6 |
| u | 13.06 | 56.52 | 25.85 | 663 | NMS4 + KMS6 + KMS4 |
| v | 9.01 | 77.47 | 24.65 | 628 | NMS4 + KMS4 + MS7 |
| i | 0 | 81.79 | 23.55 | 682 | NMS4 + MS7 |
| w | 9.04 | 79.85 | 24.2 | 619 | MS7 + KMS4 + KMCS3 |
| g | 14.71 | 0 | 21.8 | 722 | NS + N3KS |
| f | 29.68 | 0 | 6.95 | 738 | N3KS + KC |
| m | 19.37 | 49.06 | 19.38 | 678 | N3KS + KC + KMS6 |
| n | 18.62 | 52.93 | 19.5 | 669 | KC + KMS6 + KMS4 |
| p | 11.38 | 75.89 | 18.31 | 623 | KC + KMS4 + KMCS3 |
| x | 4.28 | 91.69 | 15.15 | 595 | MS7 + MS6 + KMCS3 |
| j | 0 | 94.64 | 14.25 | 596 | MS7 + MS6 |
| q | 7 | 88.32 | 6.3 | 598 | KC + KMCS3 + KMC6 |
| z | 0.34 | 99.02 | 1.04 | 475 | MC6 + MS1 + KMC6 |
| l | 0 | 99.1 | 1.25 | 476 | MC6 + MS1 |
| a | 0 | 99.25 | 0 | 480 | MC6 |
| e | 6.91 | 88.04 | 0 | 615 | KC + KMC6 |
| b | 30.2 | 0 | 0 | 770 | KC |
| k | 0 | 96.95 | 10.6 | 540 | MS6 + MS1 |
| y | 2.21 | 96.13 | 11.05 | 552 | MS6 + MS1 + KMCS3 |
| r | 2.25 | 95.31 | 8.08 | 530 | KMCS3 + KMC6 + MS1 |
| d | 0.41 | 98.84 | 0 | 473 | MC6 + MS1 + KMC6 |

## Simulation of an extractive process

Several paths through the solubility diagram can simulate an extractive process when the initial and final states of the system are known. Each of them is decomposed in elementary steps where a single variable (temperature, composition) is modified, and a mass balance is set step-by-step. Then the flow-charts of the various paths are drawn and compared in order to select the best theoretical process. A pilot unit can then be considered in order to check and adjust the conclusions of the theoretical study. The principle of simulation is illustrated in Fig. 1, where an overall process $N^{\text{init}}N^{\text{fin}}$ is decomposed in three steps: cooling (1), precipitation of salt A (2), precipitation of salt B (3).

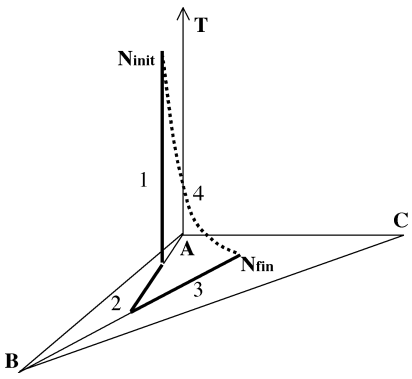


**Fig. 1** Simulation of a path through a system ABC.

## TREATMENT OF BLACK SEA WATER

### Recovery of sodium chloride by isothermal evaporation at 25 °C

The brine's composition is converted using the Jänecke expression and reported on the phase diagram. At 25 °C, the salt composition is inside the NaCl solubility field of NaCl, but the water content is outside since the solution is dilute.

#### *Saturation of NaCl*

The first step of evaporation corresponds to a variation of the water content, without change of the salt composition, until the solution becomes saturated in sodium chloride. The calculation is developed in previous publications [9,10]. Equation 2 relates the relative amount of evaporated water to the variation of the water coordinate, during the step:

$$(n_0 - n)/n_0 = (Z_0 - Z)/Z_0 \tag{2}$$

where $n_0$ and $n$ are the water amounts at the beginning and during the step. At the end-point $N_1$ the water coordinate $Z_1$ is evaluated from the sections at constant water content of the solubility phase diagram.

Figure 2 shows the sections at constant water content, and Fig. 3 presents the vertical section of the diagram containing $N_1$.

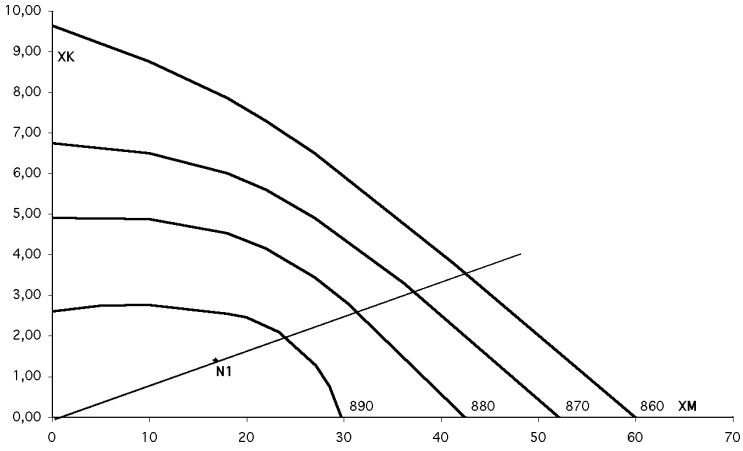


**Fig. 2** Water amount of the saturated solution (horizontal projection).

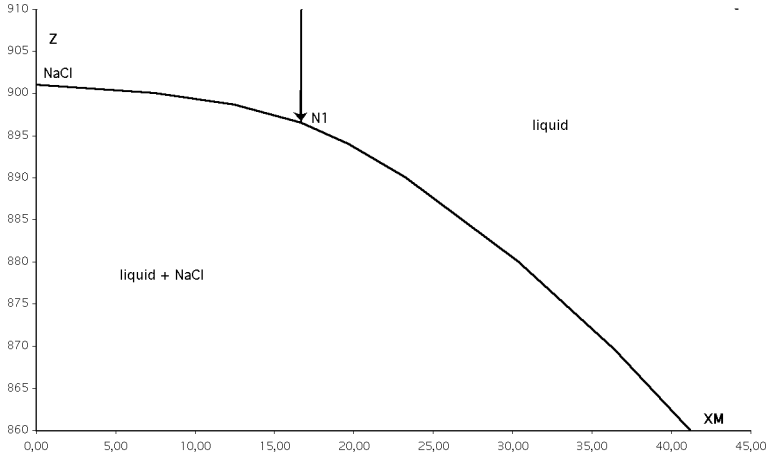


**Fig. 3** Water amount of saturated solution (vertical section).

## Crystallization sequence

### *Precipitation of pure NaCl*

The second step of evaporation is the precipitation of sodium chloride. According to the lever rule, the representative point of salt composition moves along the line NaCl–$N_1$, and a second solid appears when the representative point of the solution reaches a face of the solubility field of NaCl (point $N_2$). The calculation of $N_2$ coordinates [9,10] shows that the second observed salt is astrakanite (bloedite) $Na_2SO_4{\cdot}MgSO_4{\cdot}4H_2O$. The moving of the representative point is presented in Fig. 4.

Experimental studies mention that the metastable phase $MgSO_4{\cdot}7H_2O$ (epsomite) is obtained during natural evaporation at 25 °C [12–14]. The end-point *P* (Fig. 4) is the intersect of the line NaCl–$N_1$ with the epsomite solubility field, beyond the stable area. NaCl yield and the amount of evaporated water are presented in Table 3, for stable and metastable equilibria.

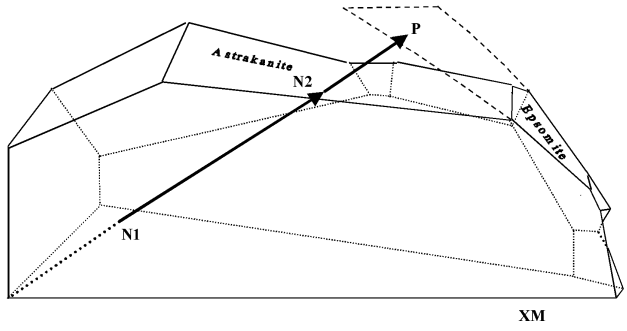


**Fig. 4** Black Sea water crystallization of pure NaCl.

**Table 3** Coprecipitation at 25 °C of NC and MS7 or NMS4.

| Composition | XM | XK | YS | Z |
|---|---|---|---|---|
| N0 | 16.7 | 1.55 | 9.37 | 18035.13 |
| N1 | 16.7 | 1.55 | 9.37 | 896.5 |
| N2 | 48.31 | 4.48 | 27.10 | 701.54 |
| P | 61.07 | 5.67 | 34.26 | 731.52 |
| N3 | 77.74 | 8.44 | 24.58 | 631.42 |

*Coprecipitation of two salts*

During the next step, the representative point of brine moves along the solubility surface of the second salt. According to the lever rule, the path through the diagram is the intersect of this surface with the plane based on the representative points of NaCl, the second salt (NMS4 or MS7) and the saturated solution ($N_2$ or $P$) [10]. The calculations, performed for stable and metastable equilibria, are presented in Table 3.

Figures 5 and 6 show the moving of the saturated solution representative point during the third step of evaporation, for stable and metastable equilibria. The end-point $N_3$ of the stable equilibrium is very close to the apex $v$ where astrakanite, leonite (KMS4), and epsomite coprecipitate with the sodium chloride. The end-point of the path $PQ$ cannot be determined due to the lack of data in the metastable field of the diagram.

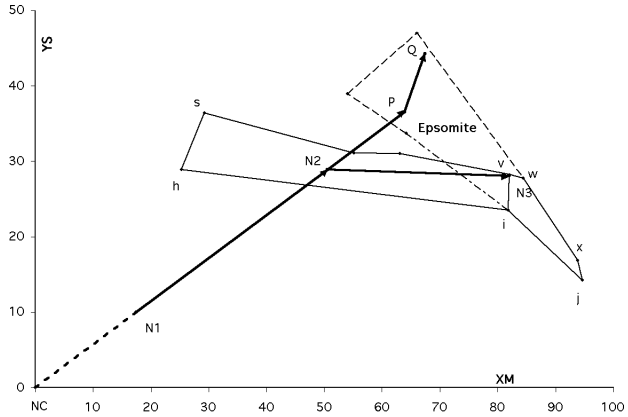


**Fig. 5** Evaporation of Black Sea water (salt composition).

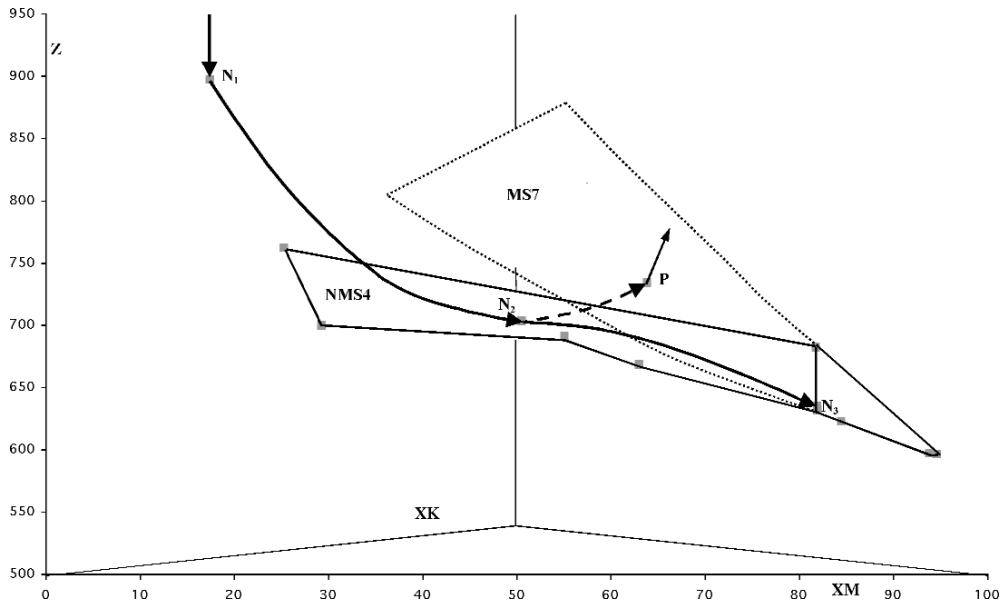


**Fig. 6** Evaporation of Black Sea water (water composition).

### *Coprecipitation of three or four salts*

At this stage of evaporation, the number and the nature of the observed solid phases depend on the experimental procedure [10,12]. If the phase equilibrium is obtained, the representative point of saturated solution moves along the edge *i*-*v* of the phase diagram. NC, NMS4, and MS7 are simultaneously observed until the representative point reaches an apex (*v*) of the diagram. Then a new solid phase (leonite, KMS4) begins to deposit and astrakanite is progressively dissolved. When the dissolution is complete, the representative point moves again along the edge *v*-*w*, etc. As already mentioned [10], the phase equilibrium is not observed for natural solar evaporation, and the representative point does not move along the edge *i*-*v*, but enters directly in the solubility field of NC + MS7.

## POSSIBLE IMPROVEMENTS OF THE EXTRACTION PROCESS

The balance of evaporation summarized in Fig. 7 shows that the mass of solution at the end of step $N_1$–$N_2$ is reduced to 1.90 % of the initial brine and contains, for 1000 Kg of NaCl precipitate:

| | |
|---|---|
| NaCl | 243.7 Kg |
| Mg (evaluated as $MgSO_4$) | 262.4 Kg |
| K (evaluated as KCl) | 30.2 Kg |

The residual brine is often rejected at this stage of evaporation, but the phase diagram suggests various treatments for the increase of sodium chloride yield or for the recovery of valuable components of the brine. These improvements can be obtained by addition of a suitable reactant, by continuation of the treatment under other conditions of temperature, and/or by cycling of brine after partial treatment. Two examples are developed, as follows.

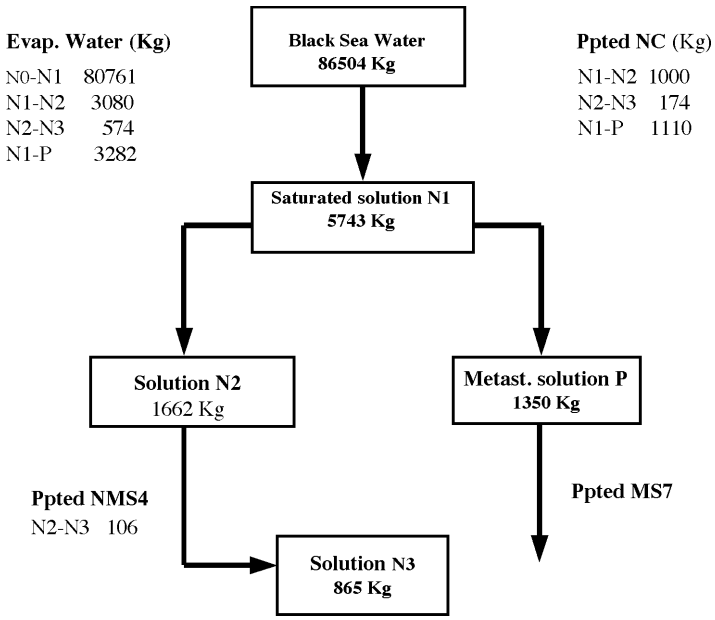


**Fig. 7** Balance of evaporation.

### Increase of the NaCl yield

During the second step of evaporation, the relative amount of NaCl precipitate is given by the relation:

$$(n_{NC}{}^{0} - n_{NC})/n_{nc}{}^{0} = 1 - \mathrm{XN}\cdot\mathrm{XK}^{0} / (\mathrm{XN}^{0}\cdot\mathrm{XK}) \quad (3)$$

The vertical section of NaCl solubility field containing $N_1$ shows (Fig. 8) that the end-point $N_2$ moves towards higher $Mg^{2+}$ concentrations when the sulfate content of the solution decreases. Consequently, the yield of sodium chloride increases, as shown in Fig. 9 and Table 4, presenting the variation of NaCl yield vs. the relative decrease of sulfate in the solution.

A 50 % diminution of the sulfate amount allows a 20 % increase of pure NaCl production. This reduction can be obtained, for example, by addition of calcium chloride to solution $N_1$ and separation of the precipited calcium sulfate.

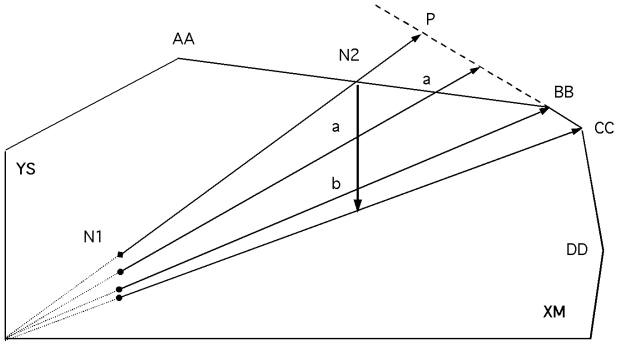


**Fig. 8** Influence of sulfate on the yield of pure NaCl. Vertical section of the solubility diagram.

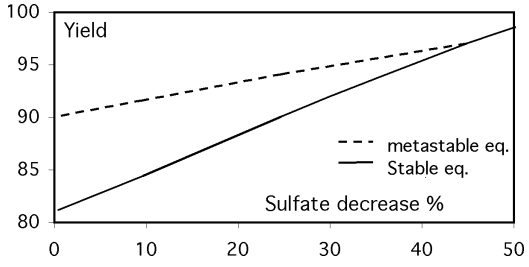


**Fig. 9** Variation of NaCl yield vs. the sulfate decrease.

**Table 4** NaCl yield, influence of sulfate.

| Sulfate decrease % | Yield | | Increase | |
|---|---|---|---|---|
| | stable eq. | metast. eq. | stable eq. | metast. eq. |
| 0 | 80 | 89.3 | 0 | 0 |
| 10 | 83.8 | 91 | 4.65 | 1.8 |
| 25 | 89.5 | 93.5 | 11.8 | 4.7 |
| 45 | 96.5 | 96.7 | 20.7 | 8.26 |
| 50 | 98 | 98 | 22.4 | 9.72 |

## Cooling of the solution

The nature of the observed solid phases depends on temperature. Figures 10 and 11 show, for example, that at 0 °C the representative point of the salt composition is located in the solubility field of mirabilite NS10, while the water content is outside, showing that the precipitate is a mixture of mirabilite and a second solid phase (sodium chloride). The nature of solids coprecipitating with mirabilite at 0 °C is presented in Table 5. The intersect of the solubility field with the vertical plane contains $N_2$.

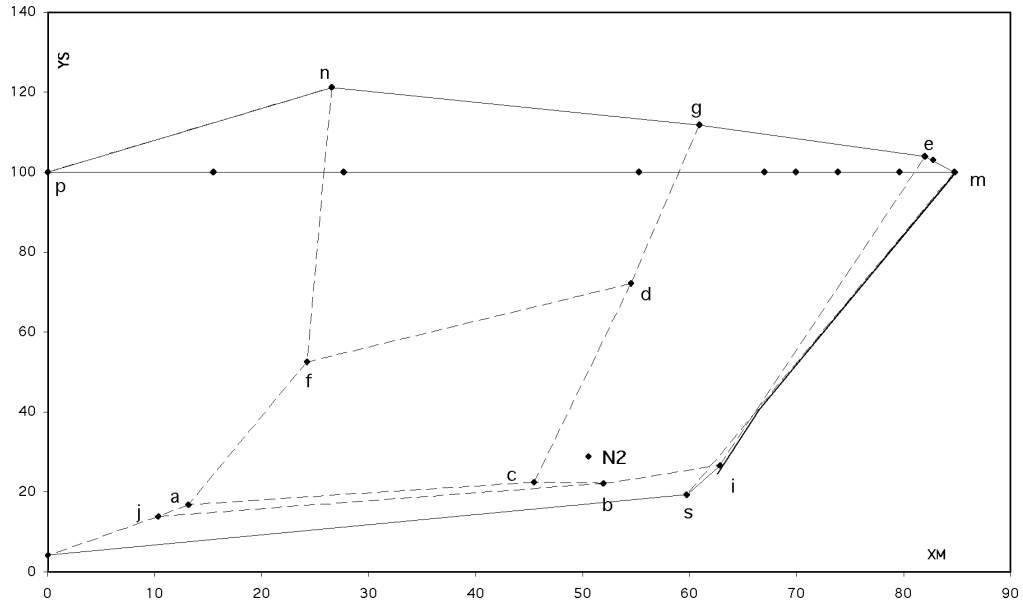


**Fig. 10** Solubility field of mirabilite at 0 °C (salt composition).

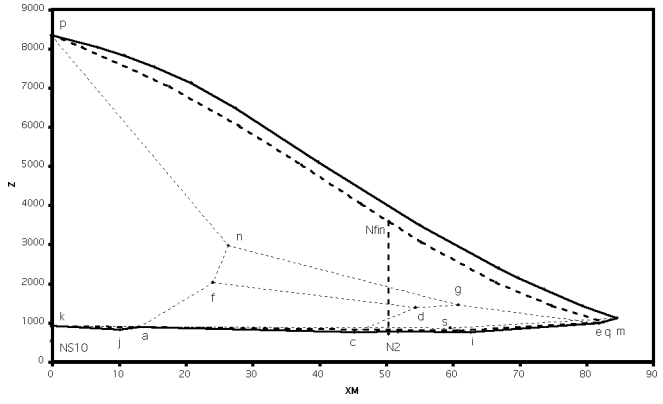


**Fig. 11** Solubility field of mirabilite (water composition).

**Table 5** Solids coprecipitating with NaCl at 0 °C.

| Face | Solid phases |
|---|---|
| kjbis | NS10 + NC |
| acbj | NS10 + KC |
| sie | NS10 + MS7 |
| bidcg | NS10 + KMS6 |
| cdfa | NS10 + N3KS |
| dhfg | NS10 + MS1 |

It is possible to recover pure decahydrated sodium sulfate from the residual brine $N_2$ by simple addition of water before cooling. The calculation shows that pure mirabilite is obtained if the amount $h$ of added water is:

$$3.70 < h/n_H2 < 4.56 \quad (4)$$

where $n_H2$ is the content of water in the solution.

The maximum amount of pure mirabilite that can be recovered for 1000 Kg of precipited NaCl is 116.0 Kg.

## CONCLUSION

The flowchart of a process can be deduced from the solubility diagram. The calculation is fast and easy, but it depends on the reliability of solubility data and has several limitations. It does not take into account some parameters of the extraction procedure: kinetics of reactions or crystallizations occurring in the medium, possible segregation or incomplete reaction, real amounts of minor or trace elements in the residual brine due to the quantities adsorbed by precipitates or removed as impregnating solution, constraints bound to an industrial development (feasibility, cost of utilities, energy balance, etc.).

The conclusions of the theoretical study must be considered as a guide and a reference. They must be carefully checked by a complementary experimental study and eventually revised in a new theoretical approach, so that the conception and optimization of an extractive process is the result of a constant "go and come" between experience and calculation.

## ACKNOWLEDGMENT

We gratefully acknowledge the Center of Excellence in Varna for its support of this work, which has been performed in the frame of an EC Project.

## REFERENCES

1. E. Jänecke. *Z. Anorg. Chem.* **51**, 132 (1906).
2. R. Cohen-Adad. *Pure Appl. Chem.* **57***,* 255–262 (1985).
3. R. Cohen-Adad, M.-Th. Cohen-Adad, R. Ouaini, F. Getzen. *J. Chim. Phys.* **87**, 1441 (1990).
4. R. Cohen-Adad, M.-Th. Cohen-Adad, R. Ouaini. *Appl. Chem.* **1**, 1–7 (1990).
5. D. Ben Hassen-Chehimi. "Contribution à l'étude et à la modélisation des systèmes salins", Ph.D. thesis, Bizerte University (1997).
6. R. Cohen-Adad and J. W. Lorimer. *Alkali Metal and Ammonium Chloride in Water and Heavy Water,* Solubility Data Series, Vol. 47, Pergamon Press, Oxford (1991).
7. R. Cohen-Adad, J. W. Lorimer, S. L. Philips, M. Salomon. *Chem. Info. Comp. Sci.* **35***,* 675–696 (1991).

8. R. Cohen-Adad, M.-Th. Cohen-Adad, D. Chehimi, A. Marrouche. In *Thermodynamical Modeling and Materials Data Engineering*, J. P. Caliste, A. Truyol, J. Westbrooke (Eds.), pp. 95–108, Springer, Berlin (1998).
9. L. Zayani. "Etude d'une saumure du sud tunisien. Séquence de cristallisation et modélisation", Ph.D. thesis, Tunis University (1999).
10. R. Cohen-Adad, M.-Th. Cohen-Adad, C. Balarew, S. Tepavitcharova, W. Voigt, L. Zayani, D. Ben Hassen-Chehimi, S. Mançour-Billah. *Monatsh. Chem.* **131**, 25–37 (2000).
11. E. Uskowski and M. Dietzel. *Atlas and Data of Solid-Solution Equilibria of Marine Evaporite*, Springer, Berlin (1998).
12. Chr. Balarev. *Russ. J. Gen. Chem*. **27**, 37–39 (1957).
13. Chr. Balarew, D. Rabadjieva, S. Tepavitcharova. *Extraction of Salts from the Sea-salt Production Waste Brines*, XXVIII Jeep, Agadir (2002).
14. R. Cohen-Adad, S. Mançour-Billah, B. Cohen-Adad. *17$^{th}$ International CODATA Conference,* Baveno (1999).
15. S. Mançour-Billah. "Modélisation et exploitation des diagrammes de phases. Application à l'étude de systèmes multi-constituants simples ou réciproques", Ph.D. thesis, University Ibn Zohr Agadir (2001).